Annals of Botany **110**: 787–795, 2012
doi:10.1093/aob/mcs153, available online at www.aob.oxfordjournals.org

ANNALS OF BOTANY
Founded 1887

Disorganization of F-actin cytoskeleton precedes vacuolar disruption in pollen tubes during the *in vivo* self-incompatibility response in *Nicotiana alata*

Juan A. Roldán, Hernán J. Rojas and Ariel Goldraij*

Centro de Investigaciones en Química Biológica de Córdoba (CIQUIBIC–CONICET), Departamento de Química Biológica, Facultad de Ciencias Químicas, Universidad Nacional de Córdoba, X5000HUA, Córdoba, Argentina
** For correspondence. E-mail arielg@fcq.unc.edu.ar*

Received: 26 December 2011 Returned for revision: 6 March 2012 Accepted: 3 May 2012 Published electronically: 9 July 2012

• *Background and Aims* The integrity of actin filaments (F-actin) is essential for pollen-tube growth. In S-RNase-based self-incompatibility (SI), incompatible pollen tubes are inhibited in the style. Consequently, research efforts have focused on the alterations of pollen F-actin cytoskeleton during the SI response. However, so far, these studies were carried out in *in vitro*-grown pollen tubes. This study aimed to assess the timing of *in vivo* changes of pollen F-actin cytoskeleton taking place after compatible and incompatible pollinations in *Nicotiana alata*. To our knowledge, this is the first report of the *in vivo* F-actin alterations occurring during pollen rejection in the S-RNase-based SI system.
• *Methods* The F-actin cytoskeleton and the vacuolar endomembrane system were fluorescently labelled in compatibly and incompatibly pollinated pistils at different times after pollination. The alterations induced by the SI reaction in pollen tubes were visualized by confocal laser scanning microscopy.
• *Key Results* Early after pollination, about 70 % of both compatible and incompatible pollen tubes showed an organized pattern of F-actin cables along the main axis of the cell. While in compatible pollinations this percentage was unchanged until pollen tubes reached the ovary, pollen tubes of incompatible pollinations underwent gradual and progressive F-actin disorganization. Colocalization of the F-actin cytoskeleton and the vacuolar endomembrane system, where S-RNases are compartmentalized, revealed that by day 6 after incompatible pollination, when the pollen-tube growth was already arrested, about 80 % of pollen tubes showed disrupted F-actin but a similar percentage had intact vacuolar compartments.
• *Conclusions* The results indicate that during the SI response in *Nicotiana*, disruption of the F-actin cytoskeleton precedes vacuolar membrane breakdown. Thus, incompatible pollen tubes undergo a sequential disorganization process of major subcellular structures. Results also suggest that the large pool of S-RNases released from vacuoles acts late in pollen rejection, after significant subcellular changes in incompatible pollen tubes.

Key words: Confocal microscopy, F-actin cytoskeleton, *Nicotiana alata*, pollen tube, self-incompatibility, S-RNase, vacuolar system.

INTRODUCTION

The cytoskeleton of actin is an essential component of the polar cell growth machinery of pollen tubes (Cheung and Wu, 2008). As in few other examples of tip growth in nature, such as root hairs in plants, hyphae in fungi and neurites in animals, actin filaments (F-actin) in normally growing pollen tubes exhibit a characteristic organization. Long cables of polymerized F-actin are arranged in parallel to the major axis of the cell. These bundles of F-actin extend in the cytoplasm from the subapical region along the shank of the pollen tube. In the subapical region, shorter and randomly disposed F-actin fragments form the 'collar zone', a dense mesh of actin immediately behind the apex (Geitmann *et al.*, 2000; Vidali *et al.*, 2001). The apical zone posseses individual and fine filaments of actin, difficult to observe and mostly under the limit of resolution for light microscopy (Staiger *et al.*, 2010). This highly structured organization of F-actin provides the appropriate frame for vesicle and organelle motility, including the transport to and from the apex of secretory vesicles, necessary to sustain the tip growth (Staiger *et al.*, 1994; Cai and Cresti, 2009). Given that pollen tubes germinate and grow easily in culture medium, most studies of F-actin organization and dynamics have been made in *in vitro* systems. However, some *in vivo* studies performed in pollen tubes growing through the style have confirmed the F-actin general disposition (Geitmann *et al.*, 2000; Chen *et al.*, 2002).

Self-incompatibility (SI) is a genetic mechanism controlled by the *S*-locus to prevent self-fertilization and the consequent inbreeding and fitness decay in plant populations (Rea and Nasrallah, 2008). SI has evolved several times in independent lineages of angiosperms and a variety of strategies are used by different plant families to stop germination or growth of incompatible pollen. At the molecular level, the best known SI mechanism is probably that of *Papaver rhoeas* which has been successfully reproduced in an *in vitro* system, mimicking *in vivo* conditions (Franklin-Tong, 2008; Poulter *et al.*, 2011). This research has revealed the crucial role of F-actin cytoskeleton during the rejection of incompatible pollen in *Papaver*. Early after SI-challenge, a massive cytoplasmic influx of free Ca^{2+} at the shank of the pollen tube triggers dramatic depolymerization of F-actin cables and subsequent formation of

punctate actin foci (Geitmann *et al.*, 2000; Snowman *et al.*, 2002; Poulter *et al.*, 2010). Moreover, F-actin depolymerization induced by SI triggers a programmed cell death (PCD) process in incompatible pollen (Thomas *et al.*, 2006; Bosch and Franklin-Tong, 2007; Wilkins *et al.*, 2011). Thus, F-actin acts as a target and effector of SI-signalling network. Changes in F-actin organization linked to induction of PCD have also been reported in animals and yeast, in several biological processes (reviewed by Franklin-Tong and Gourlay, 2008; Smertenko and Franklin-Tong, 2011).

In the S-RNase-based SI system, studied mainly in Solanaceae, Plantaginaceae and Rosaceae (Hua *et al.*, 2008; Chen *et al.*, 2010; McClure *et al.*, 2011), the role of F-actin has been considerably less studied than that of Papaveraceae. In *Pyrus pyrifolia*, *in vitro* germination and pollen-tube growth were selectively inhibited by an S-RNase of the same pollen haplotype added to the culture medium (Hiratsuka *et al.*, 2001). S-RNase caused the disruption of tip-localized reactive oxygen species; this, in turn, induced the depolymerization of F-actin, which changed from the typical axial cables to punctate actin pattern (Liu *et al.*, 2007; Wang *et al.*, 2010). These changes occurred in parallel with mitochondrial alterations and nuclear DNA degradation (Wang *et al.*, 2009) suggesting that configuration changes in F-actin would also trigger PCD during incompatible pollen rejection in Rosaceae (Wang and Zhang, 2011).

In Solanaceae, subcellular changes produced in incompatible pollen were studied early at the ultrastructural level. Morphological alterations in the rough endoplasmic reticulum, aggregation of cytoplasmic vesicles in the apex and an increase in callose deposition were reported as early manifestations of pollen rejection in *Lycopersicum peruvianum* (de Nettancourt *et al.*, 1973) and *Brugmansia suaveolens* (Geitmann *et al.*, 1995). More recently, it has been established that S-RNases were localized into vacuoles (Goldraij *et al.*, 2006; Meng *et al.*, 2009) which appear to selectively collapse after incompatible pollination, releasing the S-RNase to the cytoplasm of incompatible pollen tubes. However, no studies have been focused on the alterations of F-actin during pollen rejection in Solanaceae. On the other hand, to our knowledge, with the exception of a single experiment in *Papaver* (Geitmann *et al.*, 2000), progress in understanding configurational changes in F-actin during the SI reaction has been exclusively made in *in vitro*-cultivated pollen rather than in *in vivo*-grown pollen.

In this work, we study the alterations in the F-actin cytoskeleton of pollen tubes during the *in vivo* SI reaction in pollinated styles of *Nicotiana alata*. As the incompatible pollen tubes progressed into the style, disorganization of F-actin cables into shorter fragments gradually increased, reaching almost 80 % of the pollen tubes when they were already fully arrested. However, at this point, in >80 % of pollen tubes the vacuolar system was still well-organized. This result indicates that F-actin disorganization precedes the vacuolar breakdown during the process of incompatible pollen rejection in *Nicotiana*. Thus, incompatible pollen tubes undergo a sequential disorganization of subcellular structures, rather than an uncontrolled cytoplasmic degeneration. Consequently, it appears that the large pool of S-RNase stored in vacuoles would act late in pollen rejection, once major subcellular changes have taken place in incompatible pollen tubes. A comparison of these results with the subcellular changes in incompatible pollen tubes of *Papaver* and *Pyrus* during the *in vitro* SI response is discussed.

MATERIALS AND METHODS

Plant material, conditions of growth and pollinations

Self-incompatible *Nicotiana alata* individuals $S_{c10}S_{107}$ and $S_{70}S_{75}$, collected from a natural population previously described (Roldán *et al.*, 2010), were self-pollinated at an immature stage of pistil development to generate the homozygous genotypes $S_{c10}S_{c10}$ and $S_{70}S_{70}$, used in this work. Plants were grown in a greenhouse at 28 °C with a 16 h/8 h light/dark period.

$S_{c10}S_{c10}$ flowers were emasculated 2 d before floral maturity and pollinated 1 d after petal opening with pollen from $S_{70}S_{70}$ (compatible) or $S_{c10}S_{c10}$ (incompatible) genotypes.

Sample preparation for fluorescence microscopy

To determine the position of the pollen tube front in the style, pistils were collected at different times, stained with decolorized aniline blue and visualized by epifluorescence (Kho and Baer, 1968). For colocalization of F-actin with callose or vacuolar pyrophosphatase (vPPase), styles collected at different times were fixed for 45 min under slight vacuum with freshly prepared actin-stabilizing buffer (ASB) (Geitmann *et al.*, 2000), pH 6·8, containing 250 μM *m*-maleimidobenzoyl *N*-hydroxisuccinimide ester. Subsequently, the styles were fixed for 1 h in freshly prepared ASB containing 4 % paraformaldehyde. After three washes in ASB, 15-mm segment of a style, including the growing front of pollen tubes, was selected. Style portions were embedded at −20 °C in Cryoplast (Biopack, Argentina), cut into sections 10 μm thick in a cryostat (Leica microsystems, Germany) and put onto slides treated with 1-mM polylisine. Sections were incubated for 10 min with PBS containing 1 % each of Macerozyme R-10 (Yakult Honsha Co., Japan), Cellulase 'Onozuca' RS (Yakult Honsha Co.), and BSA. Samples were then washed three times with PBS, blocked for 30 min with PBS containing 5 % BSA and 0·1 % Triton X-100, washed again with PBS and incubated overnight with anti-callose (Biosupplies, Australia) or anti-vPPase (Goldraij *et al.*, 2006) antibodies diluted in the blocking solution with 1 % BSA. After washing three times, goat anti-mouse Alexa 546-conjugated secondary antibody (Molecular Probes, Inc.) or donkey anti-rabbit Dy Light 549-conjugated secondary antibody (Jackson Immuno Research Laboratories, Inc.) were added for 4 h to label callose or vPPase, respectively. Following two washes with PBS and one with ASB, sections were incubated overnight with 700 nM Alexa 488-conjugated phalloidin diluted in ASB containing 5 mM DTT and 0·1 % Tween 20. Specimens were washed and mounted in Fluorsave (Calbiochem, Schwalbach, Germany). For single-labelling of F-actin, the sections were incubated directly with 500 nM Alexa 488-conjugated phalloidin in the conditions described above.

Fluorescence microscopy

Confocal laser scanning fluorescence microscopy images were recorded with Zeiss LSM 5 Pascal (Carl Zeiss, Oberkochen, Germany). To detect Alexa 488, samples were scanned by argon laser (excitation 488 nm; emission, filter BandPass of 505–530 nm). Alexa 546 and DyLight 549 were detected by using helium-neon laser (excitation 543 nm; emission, long pass 560 nm). Samples were visualized with a Plan-Apochromat ×100/1·4 NA Oil DIC objective using a ×2 digital zoom. Between 12 and 14 0·5-μm serial optical sections were acquired. The images were deconvolved using the 'advanced maximum likelihood estimation algorithm' for Cell R software (Olympus Soft Imaging Solutions, Munchen, Germany), version 3·3, set with 20 iterations and an overlay sub-volume of 10 pixels. A theoretical point spread function was used.

The F-actin and the vacuolar membranes were visualized in the subapical region, including the first 50–100 μm of the pollen tube. For quantitation, F-actin and vacuolar membranes were scored as 'organized' or 'disorganized' in at least 75 pollen tubes for each replica.

RESULTS

Pollen-tube growth in compatible and incompatible pollinations

We determined the growth rate for compatible and incompatible pollen tubes in pollinated pistils of plants derived from a natural population of *Nicotiana alata* (Fig. 1). No differences were seen within the first 12 h after pollination, when pollen-tube tips had penetrated about 5 mm into the style. Then, in the compatible cross $S_{c10}S_{c10} \times S_{70}S_{70}$, pollen tubes grew through the style at a linear rate and reached the ovary within 72 h post-pollination. Incompatible pollen tubes from self-pollinated $S_{c10}S_{c10}$ plants also grew linearly on the first 3 d after pollination and subsequently continued growing at a slightly slower rate, until growth stopped below mid-style by day 5 after pollination. Since the styles were about 69 mm in length, the average growth rate was 1·0 and 0·4 mm h^{-1} for compatible and incompatible pollen tubes, respectively.

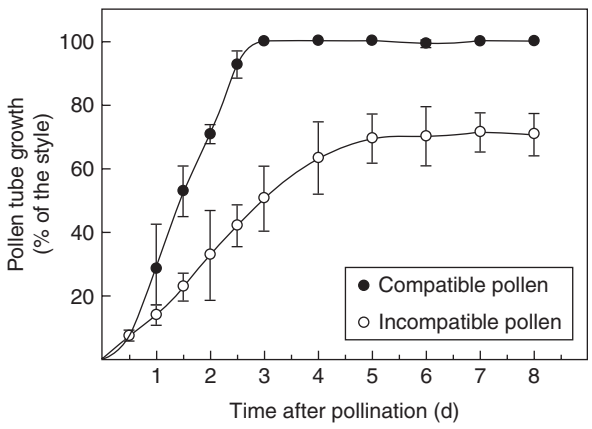

FIG. 1. Pollen-tube growth in compatible and incompatible pollinations. Pistils *Sc10Sc10* were pollinated with compatible and incompatible pollen, as indicated in the key. The position of the pollen tube front into the style was determined by epifluorescence microscopy at different times after pollination. Each point represents the mean ± s.d. of three or more independent pollinations.

F-actin pattern in compatible and incompatible pollinations

We checked first whether the fixation method used in this study was efficient to preserve F-actin disposition in *in vivo*-grown pollen tubes. Fixed sections of cross-pollinated pistils were stained with Alexa 488-phalloidin to label F-actin. The typical bundle of F-actin cables parallel to the long axis of the cell was clearly distinguished from the subapical zone to the shank (Fig. 2). A shorter filament array was seen in the ring zone, in the transition between apical and subapical regions, while the dome of the tip had fainter and disperse actin filaments. This pattern of F-actin disposition was similar to that previously reported in pollen tubes stained by different methods (Geitmann *et al.*, 2000; Wilsen *et al.*, 2006; Cheung *et al.*, 2008), confirming that the fixative procedure was appropriate to preserve F-actin organization of *in vivo*-grown pollen tubes.

Sections of cross- and self-pollinated styles collected at different times after pollination were double-labelled with phalloidin and with an antibody against callose, to stain F-actin and to demarcate the pollen tube boundaries, respectively. Representative images of compatible and incompatible pollen tubes of similar lengths are shown (Fig. 3). A similar pattern of well-organized F-actin cables was visualized 12 h after pollination (Fig. 3A, B), in consistency with the similar growth rates of compatible and incompatible pollen tubes during early pollination. In contrast, a remarkable difference was seen at a late stage of pollination. Two days after pollination, when compatible pollen tubes were in the lower style, the F-actin organization was similar to that observed in early pollination (Fig. 3C). Conversely, 5 d after incompatible pollination, when pollen growth was already arrested (see Fig. 1), F-actin had lost its normal appearance. Instead, smaller and discontinuous F-actin fragments of variable

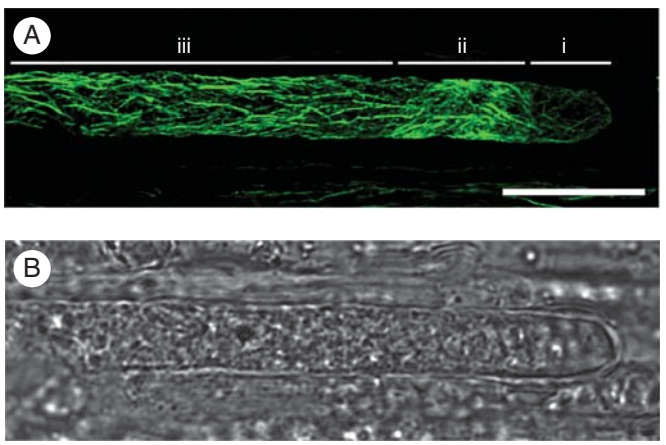

FIG. 2. F-actin cytoskeleton organization of an *in vivo*-grown pollen tube after compatible pollination. (A) Phalloidin labelling of actin (confocal projection). Three characteristic regions, from the tip to the shank, are distinguished: (i) the apex, which contains faint and short actin filaments; (ii) the collar zone, showing a brighter and dense mesh of actin; (iii) the subapex and the distal shank, showing the F-actin cables oriented parallel to the long axis of the cell. (B) Bright field of the image shown in (A). Scale bar = 10 μm.

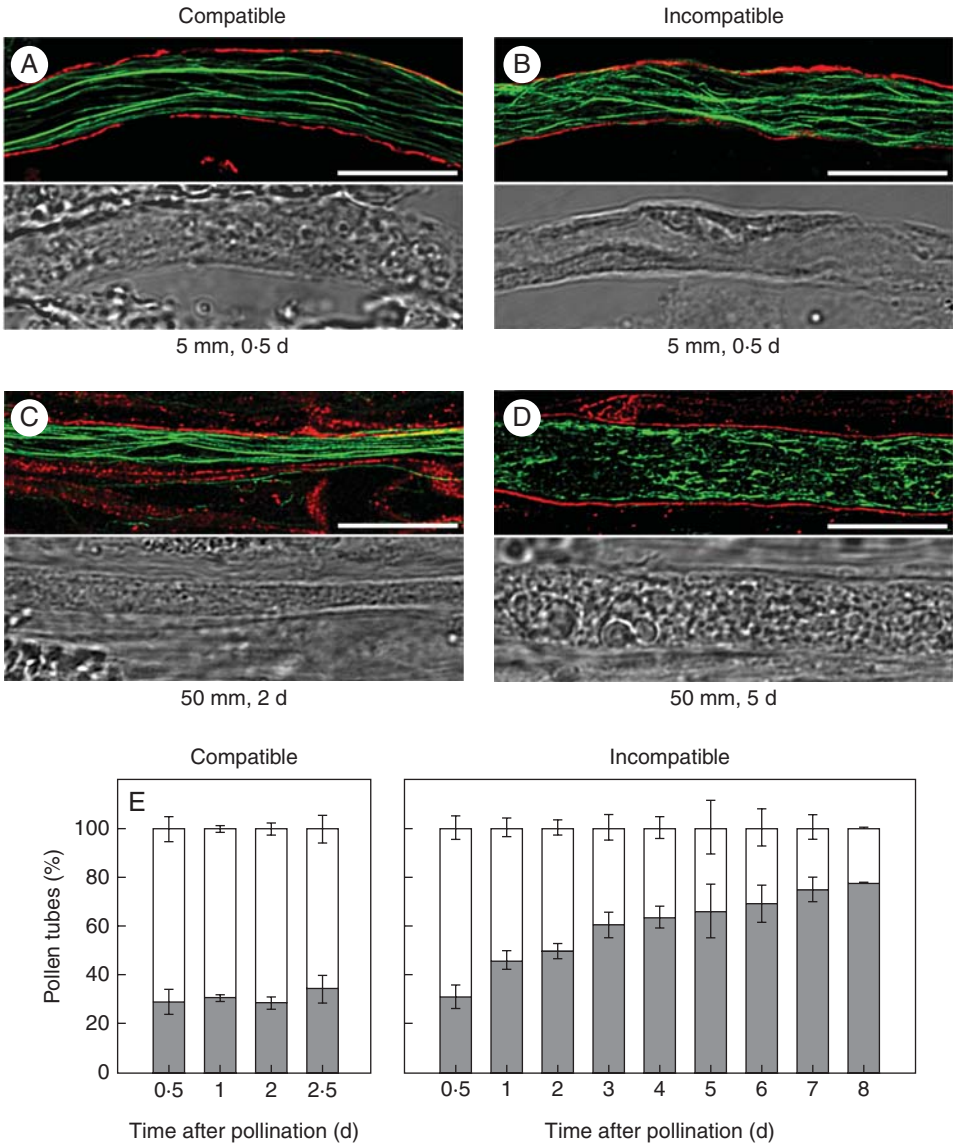

FIG. 3. Changes in the F-actin cytoskeleton of pollen tubes during the *in vivo* SI response. Colocalization of F-actin (green) and callose (red) in compatibly and incompatibly pollinated pistils. (A–D) Confocal image stack of phalloidin-stained pollen tubes was merged to the middle optical section in which callose staining demarcates the boundaries of pollen tubes (top panels); the corresponding bright fields are shown in the bottom panels. The distances from the stigma and the times after pollination are indicated below the images. Scale bar = 10 μm. (E) Quantification of F-actin morphology in compatible and incompatible pollen tubes. White, Organized actin; grey, disorganized actin. At least 75 pollen tubes were examined in each experiment. The values are the average ± s.d. for two or more independent experiments.

lengths were extended along the shank of incompatible pollen tubes (Fig. 3D). Additional images of F-actin in compatible and incompatible pollen tubes are shown in Supplementary Data Fig. S1. The two F-actin configurations shown in Fig. 3 were quantified over time for compatible and incompatible pollinations (Fig. 3E). In both types of pollinations, 30 % of pollen tubes exhibited disorganized F-actin 12 h post-pollination. While in compatible pollinations this percentage was kept constant throughout the trajectory of pollen tubes, the number of incompatible pollen tubes with disorganized F-actin exhibited a progressive increase, reaching 70 % at the time of growth arrest and almost 80 % 8 d after pollination. The pattern of F-actin disorganization shown in Fig. 3D was largely predominant at all time points after incompatible pollination. Although punctate foci of actin characteristic of *in vitro*-grown incompatible pollen tubes (Poulter *et al.*, 2010; Wang *et al.*, 2010) were occasionally observed, by day 8 after pollination they represented <13 % of pollen tubes with altered F-actin organization (Supplementary Data Fig. S2).

Disruption of F-actin cables in incompatible pollen tubes precedes vacuolar compartment disorganization

In the S-RNase-based SI system, the progression of morphological changes during incompatible pollen rejection is not fully understood. After the occurrence of early subcellular alterations, such as the excess of callose deposition, the disposition of the endoplasmic reticulum in concentric circles, and

vesicle accumulation in the apex, the degeneration of the pollen tube cytoplasm has been proposed (Geitmann, 1999; de Graaf *et al.*, 2006). On the other hand, the disorganization of vacuolar compartments, where S-RNases are confinated (Goldraij *et al.*, 2006; Meng *et al.*, 2009), has been reported as a late event during self-pollen rejection (Goldraij *et al.*, 2006). We assessed whether there was a simultaneous disorganization of F-actin bundles and the vacuolar system or, conversely, if disorganization of these major subcellular structures was carried out in a progressive and sequential manner. Colocalization experiments for F-actin cytoskeleton and the vacuolar system of pollen tubes were performed after incompatible pollinations. An antibody against vPPase was used to visualize the tonoplast of pollen vacuolar compartments. In the pollen subapical zone, these compartments were clearly defined and considerably diverse in size and morphology (Hicks *et al.*, 2004; Supplementary Data Fig. S3). Representative images of different patterns of F-actin and vacuolar membranes in incompatible pollen tubes at different days after pollination are shown in Fig. 4. Both F-actin and

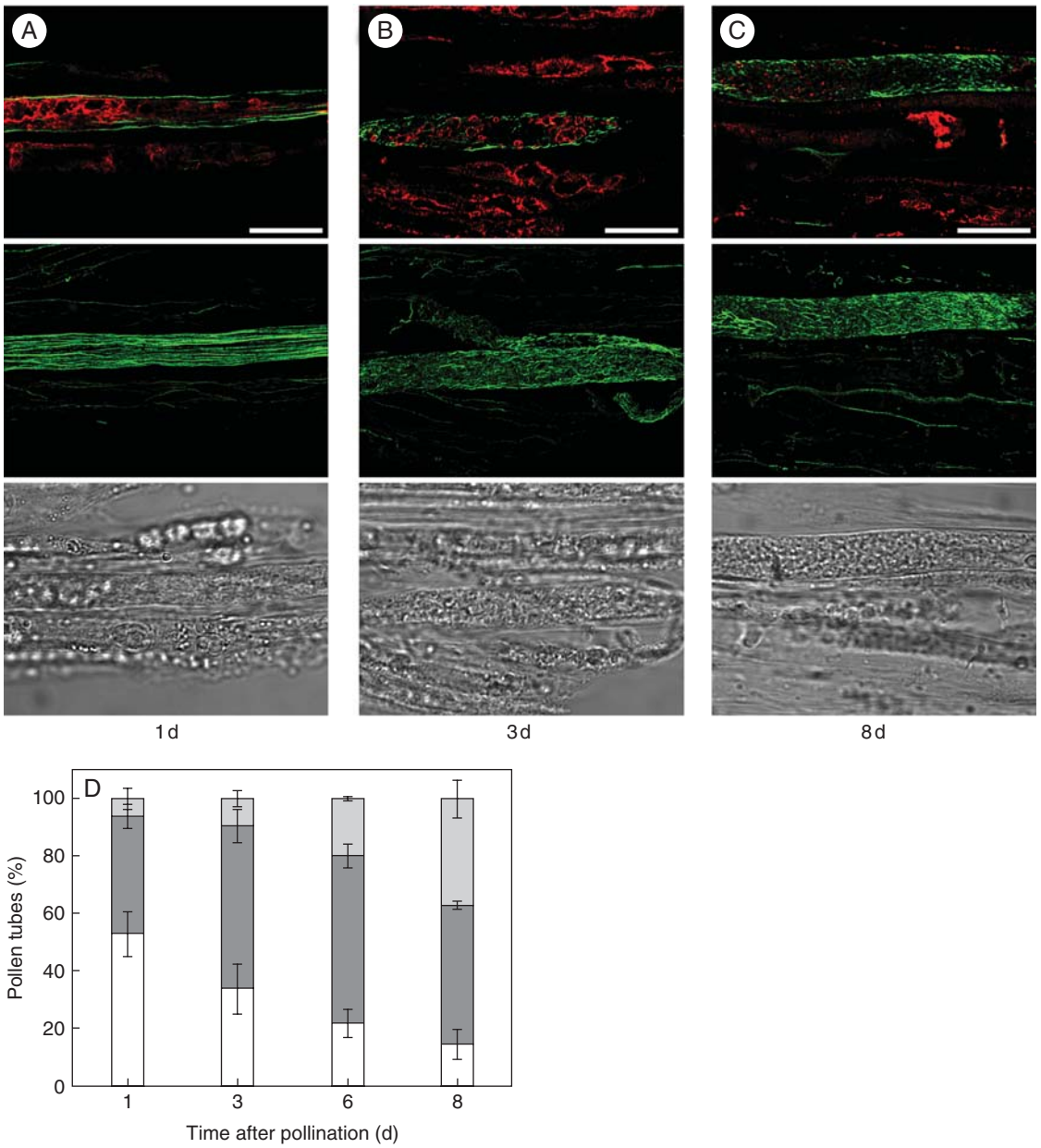

FIG. 4. Disorganization of F-actin cytoskeleton precedes vacuolar breakdown in incompatible pollen tubes during the *in vivo* SI response. Colocalization of F-actin (green) and vPPase (red) in incompatibly pollinated pistils. The images are representative of the three patterns observed: (A) organized F-actin and vacuolar endomembrane system; (B) disorganized F-actin and organized vacuolar endomembrane system; (C) disorganized F-actin and vacuolar endomembrane system. Merged optical sections (top panels), full projections of phalloidin-stained pollen tubes (central panels) and the corresponding bright fields (bottom panels) are shown. The days after pollination are indicated below the images. Scale bar = 10 μm. (D) Quantification of morphology of F-actin and vacuolar endomembrane system. White, organized F-actin and vacuolar system; dark grey, disorganized F-actin and organized vacuolar system; light grey, disorganized F-actin and vacuolar system. Seventy-five pollen tubes were examined in each experiment. The values are the average ± s.d. for two or more independent experiments.

vacuolar compartments were predominantly well-organized 1 d after pollination (Fig. 4A). Instead, by day 3 after pollination, the majority of pollen tubes showed that F-actin bundles mostly disappeared and were replaced by much smaller fragments, while the integrity of the vacuolar system appeared to be normal (Fig. 4B). By day 8 post-pollination, the loss of integrity of F-actin in individual cells was similar to that observed 3 d after pollination. Most pollen tubes still exhibited organized vacuoles; however, there was an increase in the frequency of pollen tubes in which no signal of vacuolar compartments was detected, while the vacuoles of the adjacent transmitting tissue were normally labelled (Fig. 4C). The simultaneous quantification of F-actin organization and the integrity of the vacuolar compartment in incompatible pollen tubes is shown in Fig. 4D. From day 1 to day 3 after incompatible pollination, pollen tubes with disorganized F-actin increased from 48 % to 67 %, but <8 % of pollen tubes showed both disorganized F-actin and vacuolar compartments by 3 d after pollination. By 8 d after pollination almost 70 % of pollen tubes showed intact vacuoles but >84 % of pollen tubes had disorganized F-actin. No pollen tubes with organized F-actin and disrupted vacuolar compartments were seen on any day. These results suggest strongly that F-actin disorganization occurs earlier than vacuolar breakdown during the process of incompatible pollen rejection in *Nicotiana*.

DISCUSSION

In this work we studied the *in vivo* subcellular changes of *Nicotiana alata* pollen tubes after compatible and incompatible pollinations, focusing on the organization of F-actin cytoskeleton and the vacuolar endomembrane system. We analysed the temporal sequence of alterations in incompatible pollen tubes establishing that the disorganization of F-actin occurs progressively over time and precedes vacuolar disruption, which takes place mainly after pollen-tube growth has been completely inhibited.

The highly organized disposition of F-actin cytoskeleton in pollen tubes is essential to support polar tip growth (Cheung and Wu, 2008). Longitudinal cables along the shank of the pollen tube provide the appropriate track for organelle movement and cytoplasmic streaming, while finer and shorter actin filaments in the subapical and apical zone are presumably involved in vesicle transport to the apex (Staiger *et al.*, 2010). Disruption of F-actin cytoskeleton organization causes a severe reduction or inhibition of pollen-tube growth (Gibbon *et al.*, 1999). Given the close association between actin configuration and polar growth, the alterations in the F-actin cytoskeleton of pollen tubes have been extensively studied in the SI response, during which incompatible pollen growth is inhibited. However, these studies – mainly performed on pollen tubes of *Papaver* (Geitmann *et al.*, 2000; Snowman *et al.*, 2002; for a recent review, see Poulter *et al.*, 2011) and *Pyrus* (Liu *et al.*, 2007; Wang *et al.*, 2010) – were largely conducted on *in vitro*-cultivated pollen rather than on *in vivo*-grown pollen tubes. To our knowledge, this work is the first report on the *in vivo* changes in the F-actin cytoskeleton during incompatible pollen rejection in the S-RNase-based SI system.

Typically, the site of pollen-tube arrest in Solanaceae SI is the upper third of the style (Rea and Nasrallah, 2008), although variations in this respect have been reported in *Nicotiana* (Pandey, 1979). Grafting compatibly pollinated styles onto incompatible styles, Lush and Clarke (1997) showed that pollen-tube arrest can occur in the lower part of the style, as is the case in this work (Fig. 1). Presumably, the longer growth of incompatible pollen tubes shown in Fig. 1 also occurred because the individuals used in this study have recently been derived from a natural population (Roldán *et al.*, 2010), where robustness of the SI response is quite variable (Good-Avila *et al.*, 2008).

To characterize pollen F-actin cytoskeleton during the SI reaction, we used fluorescent phalloidin to stain pollinated pistils, which had been fixed under the appropriate conditions to protect actin filaments (Doris and Steer, 1996). The general F-actin pattern we obtained, in compatible and in early stages of incompatible pollen tubes, was essentially identical to that of *in vitro*-grown pollen tubes stained with phalloidin or immunolabelled (Wilsen *et al.*, 2006) or labelled with several GFP-actin binding proteins (Cheung *et al.*, 2008). Our images are also similar to previous reports on F-actin cables imaged from pollen tubes grown in the style of lily (Jauh and Lord, 1995), tobacco (Chen *et al.*, 2002) and poppy (Geitmann *et al.*, 2000). The coincidence between the F-actin pattern visualized by a number of different techniques and the images shown in this work confirmed that the quality of the fixative procedure used in pollinated pistils of *Nicotiana* was good enough to preserve the F-actin organization of pollen tubes.

Consistent with the slow mechanism of pollen rejection in the S-RNase-based SI system, disorganization of F-actin in incompatible pollen tubes was gradual and progressive and paralleled the pollen-tube growth rate (Figs 1 and 3). The interruption of the normal configuration of F-actin cables probably impeded normal vesicle and organelle trafficking to the growing tip and caused the arrest of pollen-tube growth (Gibbon *et al.*, 1999; Chen *et al.*, 2007; Zhang *et al.*, 2010). Although F-actin disruption was reported to be not sufficient *per se* to kill the pollen tubes (Snowman *et al.*, 2002), it can act as an effector of diverse signalling cascades (Staiger, 2000; Thomas *et al.*, 2006). Thus, F-actin disorganization in *Nicotiana* could be an early manifestation at the cellular level of a more complex process leading to pollen rejection, as was reported on *Papaver* (reviewed in Franklin-Tong, 2008). To place the F-actin disruption within the time course of SI-induced alterations, actin structures were colocalized with vPPase, a tonoplast marker of the vacuolar endomembrane system. Vacuolar disruption was characterized as a late event in the SI reaction in *Nicotiana*. This is particularly relevant, since vacuoles demarcated by vPPase store the S-RNase (Goldraij *et al.*, 2006), the cytotoxic agent ultimately responsible for pollen rejection in the S-RNase-based SI systems (McClure *et al.*, 1990; Huang *et al.*, 1994). Simultaneous visualization of F-actin cytoskeleton and vacuolar membranes allowed us to establish a sequence of cellular events during pollen rejection (Fig. 4). Six days after pollination, when the incompatible pollen-tube growth was fully inhibited, about 80 % of pollen tubes exhibited disorganized F-actin structures; however, the vacuolar membrane system was still intact in 80 % of pollen tubes. Thus, during incompatible pollen rejection in *Nicotiana*, vacuole disruption occurs almost entirely after an extensive F-actin disorganization.

Ultrastructural studies in the S-RNase-based SI system revealed that incompatible and compatible pollen tubes cannot be distinguished early after pollination. The first morphological changes in the *Brugamansia* and *Lycopersicum* populations studied were visualized between 4 h and 8 h post-pollination and consisted of concentric structures in ER, accumulation of vesicles in the tube apex and thickened cell wall by the increase of callose deposition (de Nettancourt *et al.*, 1973; Geitmann *et al.*, 1995). Subsequently, a general cytoplasmic degeneration was reported to occur (Geitmann, 1999). Based on these morphological changes and the slow timing of pollen rejection, it has been suggested that a necrotic process in incompatible pollen in the S-RNase-based SI system occurs (Geitmann, 1999; Geitmann *et al.*, 2004; de Graaf *et al.*, 2006). Interestingly, both F-actin disorganization and tonoplast disruption have been described as typical alterations in many processes of plant PCD, including SI (for recent reviews, see Hara-Nishimura and Hatsugai, 2011; Smertenko and Franklin-Tong, 2011). F-actin depolymerization induced PCD during pollen rejection of incompatible pollen tubes in *Papaver* (Thomas *et al.*, 2006) through a well-studied signal-cascade (Franklin-Tong, 2008) that resulted in caspase activation and a pronounced acidification of cytosol (Bosch and Franklin-Tong, 2007). This suggested that tonoplast rupture could be involved in *Papaver* SI-reaction. Even more significant, in *Pyrus*, where pollen is rejected by the S-RNase-based SI system, extensive F-actin depolymerization was induced within 30 min after the addition of self S-RNase to *in vitro*-grown pollen tubes (Liu *et al.*, 2007; Wang *et al.*, 2010). Alterations in mitochondrial permeability, DNA degradation and tip-localized reactive-oxygen species disruption were also triggered in *Pyrus* pollen tubes by S-RNase added to the growth medium (Wang *et al.*, 2009, 2010). Since all these changes took place before pollen-growth arrest, the authors suggested that they were the cause but not the consequence of pollen inhibition (Liu *et al.*, 2007; Wang and Zhang, 2011) and proposed a cascade-signal pathway that would produce PCD in *Pyrus* pollen. In this model, RNA degradation by S-RNase could be only the beginning of the SI response (Wang and Zhang, 2011). On the other hand, the results reported here from *in vivo* experiments, show that pollen growth inhibition and F-actin disorganization occurred in parallel and preceded tonoplast disruption. Since a large pool of S-RNases is compartmentalized into pollen vacuoles (Goldraij *et al.*, 2006; Meng *et al.*, 2009), these results suggest that, in *Nicotiana*, massive RNA degradation would be a late event in the SI reaction, occurring after major cellular changes take place in rejected pollen tubes. It could be possible that this late and massive release of S-RNase was necessary to warrant the fulfilment and the irreversibility of the rejection process. However, we cannot rule out the existence of a different pool of S-RNases exerting some cytotoxic action in an early stage of pollen rejection. Recently, questions have been raised about possible differences between *in vivo* and *in vitro* mechanisms of pollen rejection in the S-RNase-based system (Zhang *et al.*, 2009; Chen *et al.*, 2010). In any case, since the nature of pollen rejection in S-RNase-based SI is complex, the exact role of S-RNase is still a matter of debate (Zhang *et al.*, 2009). Early grafting experiments conducted by Lush and Clarke (1997) showed that growth inhibition caused by incompatible styles could be reverted in some pollen tubes, suggesting that the cytotoxic effect of S-RNase was not permanent and not exclusively related to RNA degradation. In this regard, it is noteworthy that, in several T2 ribonucleases, some biological roles, including cytotoxicity, are independent of their catalytic activities (Thompson and Parker, 2009; for a review, see Luhtala and Parker, 2010). Interestingly, a fungal T2-RNase, termed ACTIBIND, exerts its cytotoxic activity by binding actin and disrupting the actin network in colon cancer cells (Roiz *et al.*, 2006). It will be crucial to know if additional roles to RNA degradation of incompatible pollen can be attributed to S-RNases.

Importantly, our results fit well the two models that currently explain pollen rejection in the S-RNase-based SI system. The S-RNase degradation and S-RNase compartmentalization models can be conciliated, since both assume that recognition and cytotoxicity take place in pollen cytoplasm, where pollen recognition factors – the SLF proteins – are localized (Wang and Xue, 2005; Meng *et al.*, 2010). A minor portion of S-RNases can gain access to the pollen cytoplasm by retrograde transport for recognizing the SLF products (Goldraij *et al.*, 2006). In incompatible pollinations, self-S-RNases and/or other still unknown factors could initiate a cytotoxic effect targeting gradually the organization of the F-actin cytoskeleton (Wang and Zhang, 2011). This in turn might trigger a cascade of signals, affecting subsequently vacuolar membrane integrity and releasing the large pool of compartmentalized S-RNases in the final steps of pollen rejection. Conversely, in compatible pollinations, degradation of ubiquitinated non-self-S-RNases by proteosome machinery (Hua *et al.*, 2008) would preserve the integrity of F-actin and vacuolar compartments, allowing the pollen tube to progress to the ovary. It is expected that non-S-specific pistil factors also contribute to regulate both compatible and incompatible scenarios, although their precise role is still unknown.

In conclusion, during the SI response in *Nicotiana*, significant subcellular changes took place in incompatible pollen tube through a sequence of time-ordered events. The normal bundles of pollen F-actin cytoskeleton were gradually disrupted, in parallel with a reduced growth rate. The breakdown of the vacuolar endomembrane system occurred subsequently, only after an extensive F-actin disorganization. These results indicated that during rejection of incompatible pollen there was a progressive rather than a rapid and uncontrolled collapse of cellular structures. This also suggested that the catalytic activity of S-RNases, which was shown to be essential for the SI response (Huang *et al.*, 1994), would manifest itself in a late stage of pollen rejection, after major cellular dismantling of incompatible pollen tubes.

SUPPLEMENTARY DATA

Supplementary data are available online at www.aob.oxfordjournals.org and consist of the following. Figure S1: changes in the F-actin cytoskeleton of pollen tubes during the *in vivo* SI response. Figure S2: punctate foci of actin in incompatible pollen tubes. Figure S3: morphological diversity of pollen tube vacuoles.

ACKNOWLEDGEMENTS

We thank Dr Jorge Muschietti and Dr Carlos Argaraña for critically reading the manuscript, Dr Carlos Mas and Dr Cecilia Sampedro for their assistance in digital image processing, and Gabriela Diaz Cortez for editorial and language assistance. This work was supported by Agencia Nacional de Promoción Científica y Tecnológica (PICT 32933); Consejo Nacional de Investigaciones Científicas y Tecnológicas (PIP 11220090100265); and SECyT – Universidad Nacional de Córdoba (05/C466) to A.G.

LITERATURE CITED

Bosch M, Franklin-Tong VE. 2007. Temporal and spatial activation of a caspase-like enzymes induced by self-incompatibility in *Papaver* pollen. *Proceedings of the National Academy of Sciences of the USA* **104**: 18327–18332.

Cai G, Cresti M. 2009. Organelle motility of pollen tube: a tale of 20 years. *Journal of Experimental Botany* **60**: 495–508.

Chen CY, Wong EI, Vidali L, *et al*. 2002. The regulation of actin organization by actin-depolymerizing factor in elongating pollen tubes. *The Plant Cell* **14**: 2175–2190.

Chen T, Teng N, Wu X, *et al*. 2007. Disruption of actin filaments by latrunculin B affects cell wall construction in *Picea meyeri* pollen tube by disturbing vesicle trafficking. *Plant Cell Physiology* **48**: 19–30.

Chen G, Zhang B, Zhao Z, Sui Z, Zhang H, Xue Y. 2010. 'A life or death decision' for pollen tubes in S-RNase-based self-incompatibility. *Journal of Experimental Botany* **61**: 2027–2037.

Cheung AY, Wu HM. 2008. Structural and signaling networks for the polar cell growth machinery in pollen tubes. *Annual Review of Plant Biology* **59**: 547–572.

Cheung AY, Duan Qh, Santos Costa S, *et al*. 2008. The dynamic pollen tube cytoskeleton: live cell studies using actin-binding and microtubule-binding reporter proteins. *Molecular Plant* **1**: 686–702.

Doris FP, Steer MW. 1996. Effects of fixatives and permeabilisation buffers on pollen tubes: implications for localisation of actin microfilaments using phalloidin staining. *Protoplasma* **195**: 25–36.

Franklin-Tong VE. 2008. Self-incompatibility in *Papaver rhoeas*: progress in understanding mechanisms involved in regulating self-incompatibility in *Papaver*. In: Franklin-Tong VE. ed. *Self-incompatibility in flowering plants: evolution, diversity and mechanisms.* Berlin: Springer, 237–258.

Franklin-Tong VE, Gourlay CW. 2008. A role for actin in regulating apoptosis/programmed cell death: evidence spanning yeast, plants and animals. *Biochemical Journal* **413**: 389–404.

Geitmann A, Hudák J, Vennigerholz F, Walles B. 1995. Immunogold localization of pectine and callose in pollen grains and pollen tubes of *Brugmansia suaveolens*: implications for the self-incompatibility reaction. *Journal of Plant Physiology* **147**: 225–235.

Geitmann A. 1999. Cell death of self-incompatible pollen tubes: necrosis or apoptosis? In: Cresti M, Cai G, Moscatelli A eds. *Fertilization in higher plants: molecular and cytological aspects*. Berlin: Springer, 113–137.

Geitmann A, Snowman BN, Emons AMC, Franklin-Tong VE. 2000. Alterations in the actin cytoskeleton of pollen tubes are induced by the self-incompatibility reaction in *Papaver rhoeas*. *The Plant Cell* **12**: 1239–1251.

Geitmann A, Franklin-Tong VE, Emons AC. 2004. The self-incompatibility response in *Papaver rhoeas* pollen causes early and striking alterations to organelles. *Cell Death and Differentiation* **11**: 812–822.

Gibbon BC, Kovar DR, Staiger CJ. 1999. Latrunculin B has different effects on pollen germination and tube growth. *The Plant Cell* **11**: 2349–2364.

Goldraij A, Kondo K, Lee CB, *et al*. 2006. Compartmentalization of S-RNase and HT-B degradation in self-incompatible *Nicotiana*. *Nature* **439**: 805–810.

Good-Avila SV, Mena-Alí JI, Stephenson AG. 2008. Genetic and environmental causes and evolutionary consequences of variations in self-fertility in self-incompatible species. In: Franklin-Tong VE. ed. *Self-incompatibility in flowering plants: evolution, diversity and mechanisms.* Berlin: Springer, 33–51.

de Graaf BHJ, Lee C, McClure BA, Franklin-Tong VE. 2006. Cellular mechanisms for pollen tube growth inhibition in gametophytic self-incompatibility. In: Malhó R. ed. *The pollen tube*. Berlin: Springer, 201–221.

Hara-Nishimura I, Hatsugai N. 2011. The role of vacuole in plant cell death. *Cell Death and Differentiation* **18**: 1298–1304.

Hicks GR, Rojo E, Hong S, Carter DC, Raikhel NV. 2004. Germinating pollen has tubular vacuoles, displays highly dynamic vacuole biogenesis, and requires *VACUOLESS1* for proper function. *Plant Physiology* **134**: 1227–1230.

Hiratsuka S, Zhang SL, Nakagawa E, Kawai Y. 2001. Selective inhibition of the growth of incompatible pollen tubes by S-protein in the Japanese pear. *Sexual Plant Reproduction* **13**: 209–215.

Hua Z, Fields A, Kao T-h. 2008. Biochemical models for S-RNase-based self-incompatibility. *Molecular Plant* **1**: 575–585.

Huang S, Lee HS, Karunandaa B, Kao T-h. 1994. Ribonuclease activity of *Petunia inflata* S proteins is essential for rejection of self-pollen. *The Plant Cell* **6**: 1021–1028.

Jauh GY, Lord EM. 1995. Movement of the tube cell in the lily style in the absence of the pollen grain and the spent pollen tube. *Sexual Plant Reproduction* **8**: 168–172.

Kho YO, Baer J. 1968. Observing pollen tubes by means of fluorescence. *Euphytica* **17**: 299–302.

Liu Zq, Xu Gh, Zhang Sl. 2007. *Pyrus pyrifolia* stylar S-RNase induces alterations in the actin cytoskeleton in self-pollen and tubes *in vitro*. *Protoplasma* **232**: 61–67.

Luhtala N, Parker R. 2010. T2 family ribonucleases: ancient enzymes with diverse roles. *Trends in Biochemical Sciences* **35**: 253–259.

Lush MW, Clarke AE. 1997. Observations of pollen tube growth in *Nicotiana alata* and their implications for the mechanism of self-incompatibility. *Sexual Plant Reproduction* **10**: 27–35.

McClure BA, Gray JE, Anderson MA, Clarke AE. 1990. Self-incompatibility in *Nicotiana alata* involves degradation of rRNA. *Nature* **347**: 757–760.

McClure BA, Cruz-García F, Romero C. 2011. Compatibility and incompatibility in S-RNase-based systems. *Annals of Botany* **108**: 647–658.

Meng XY, Hua ZH, Wang N, Fields AM, Dowd PE, Kao T-h. 2009. Ectopic expression of S-RNase of *Petunia inflata* in pollen results in its sequestration and non-cytotoxic function. *Sexual Plant Reproduction* **22**: 263–275.

Meng XY, Sun P, Kao T-H. 2010. S-RNase-based self-incompatibility in *Petunia*. *Annals of Botany* **108**: 637–646.

de Nettancourt D, Devreux M, Bozzini A, Cresti M, Pacini E, Sarfatti G. 1973. Ultrastructural aspects of the self-incompatibility mechanism in *Lycopersicum peruvianum* Mill. *Journal of Cell Science* **12**: 403–419.

Pandey KK. 1979. The genus *Nicotiana*: evolution of incompatibility in flowering plants. In: Hawkes JG, Lester RN, Skelding AD. eds. *The biology and taxonomy of the Solanaceae*. London: Academic Press, 421–434.

Poulter NS, Staiger CJ, Rappoport JZ, Franklin-Tong VE. 2010. Actin-binding proteins implicated in the formation of the punctate actin foci stimulated by the self-incompatibility response in *Papaver*. *Plant Physiology* **152**: 1274–1283.

Poulter NS, Bosch M, Franklin-Tong VE. 2011. Proteins implicated in mediating self-incomaptibility-induced alterations to the actin cytoskeleton of *Papaver* pollen. *Annals of Botany* **108**: 659–675.

Rea AC, Nasrallah JB. 2008. Self-incompatibility systems: barriers to self-fertilization in flowering plants. *International Journal of Developmental Biology* **52**: 627–636.

Roiz L, Smirnoff P, Bar-Eli M, Schwartz B, Shoseyov O. 2006. ACTIBIND, an actin-binding fungal T2-RNase with antiangiogenic and anticarcinogenic characteristics. *Cancer* **106**: 2295–2308.

Roldán JA, Quiroga R, Goldraij A. 2010. Molecular and genetic characterization of novel *S-RNases* from a natural population of *Nicotiana alata*. *Plant Cell Reports* **29**: 735–746.

Smertenko A, Franklin-Tong VE. 2011. Organisation and regulation of the cytoskeleton in plant programmed cell death. *Cell Death and Differentiation* **18**: 1263–1270.

Snowman BN, Kovar DR, Shevchenko G, Franklin-Tong VE, Staiger CJ. 2002. Signal-mediated depolymerization of actin in pollen during the self-incompatibility response. *The Plant Cell* **14**: 2613–2626.

Staiger CJ. 2000. Signaling to the actin cytoskeleton in plants. *Annual Review of Plant Physiology and Plant Molecular Biology* **51**: 257–288.

Staiger CJ, Yuan M, Valenta R, Shaw PJ, Warn RM, Lloyd CW. 1994. Microinjected profilin affects cytoplasmic streaming in plant cells by

rapidly depolymerizing actin microfilaments. *Current Biology* **4**: 215–219.

Staiger CJ, Poulter NS, Henty JL, Franklin-Tong VE, Blanchoin L. 2010. Regulation of actin dynamics by actin-binding proteins in pollen. *Journal of Experimental Botany* **61**: 1969–1986.

Thomas SG, Huang S, Li S, Satiger CJ, Franklin-Tong VE. 2006. Actin depolymerization is sufficient to induce programmed cell death in self-incompatible pollen. *Journal of Cell Biology* **174**: 221–229.

Thompson DM, Parker R. 2009. The RNase Rny1p cleaves tRNAs and promotes cell death during oxidative stress in *Saccharomyces cerevisiae*. *Journal of Cell Biology* **185**: 43–50.

Vidali L, McKenna ST, Hepler PK. 2001. Actin polymerization is essential for pollen tube growth. *Molecular Biology of the Cell* **12**: 2534–2545.

Wang CL, Zhang SL. 2011. A cascade signal pathway occurs in self-incompatibility of *Pyrus pyrifolia*. *Plant Signaling & Behavior* **6**: 420–421.

Wang CL, Xu GH, Jiang XT, *et al*. 2009. S-RNase triggers mitochondrial alteration and DNA degradation in the incompatible pollen tube of *Pyrus pyrifolia in vitro The Plant Journal* **57**: 220–229.

Wang CL, Wu J, Xu GH, *et al*. 2010. S-RNase disrupts tip-localized reactive oxygen species and induces nuclear DNA degradation in incompatible pollen tubes of *Pyrus pyrifolia*. *Journal of Cell Science* **123**: 4301–4309.

Wang HY, Xue YB. 2005. Subcellular localization of the *S* locus F-box protein AhSLF-S_2 in pollen and pollen tubes of self-incompatible *Antirrhinum*. *Journal of Integrative Plant Biology* **47**: 76–83.

Wilkins KA, Bancroft J, Bosch M, Ings J, Smirnoff N, Franklin-Tong VE. 2011. Reactive oxygen species and nitric oxide mediate actin reorganization and programmed cell death in the self-incompatibility response of *Papaver*. *Plant Physiology* **156**: 404–416.

Wilsen KL, Lovy-Wheeler A, Voigt B, Menzel D, Kunkel JG, Hepler PK. 2006. Imaging the actin cytoskeleton in growing pollen tubes. *Sexual Plant Reproduction* **19**: 51–62.

Zhang Y, Zhao Z, Xue Y. 2009. Roles of proteolysis in plant self-incompatibility. *Annual Review of Plant Biology* **60**: 21–42.

Zhang Y, He J, Lee D, McCormick S. 2010. Interdependence of endomembrane trafficking and actin dynamics during polarized growth of *Arabidopsis* pollen tubes. *Plant Physiology* **152**: 2200–2210.